

A98-31716

METHODOLOGY FOR CONCEPTUAL DESIGN AND OPTIMISATION OF TRANSPORT AIRCRAFT

Askin T. Isikveren*, Aircraft Performance Engineer
American Airlines, Fort Worth, Texas

Abstract

This paper presents techniques for conducting and subsequently optimising new transport aircraft designs at the conceptual level with an emphasis placed on turbofan vehicles ranging in size from 19 to 100 passengers as well as business jets. The method is comprised of the discrete operations usually performed for a conventional (intuitive) design process but combines it with a non-hierarchical multidisciplinary optimisation philosophy. A new unified analytical treatment of the design problem is presented which utilises closed form solutions together with transcendental expressions. These methods cover: installed powerplant modelling, high and low speed aerodynamics, minimum control speed limited balanced field estimation, and, the formulation of operational performance characteristics such as definition of speed schedules and techniques for payload-range/sector flight profile optimisation with regards to maximum specific range, minimum fuel, maximum block speed, minimum time, minimum direct operating cost and maximum return on investment. A design study has been performed with a spreadsheet based version of the theory and methodology. With the aid of QCARD or Quick Conceptual Aircraft Research and Development, a new 31-34 passenger regional turbofan transport was presented with lower acquisition cost and competitive weight, field and enroute performance attributes compared to its contemporaries.

Introduction

Contemporary conceptual design methodology primarily focuses on a variety of closed form expressions to enable prediction of aircraft geometry, weight, aerodynamics and field-enroute performance. Simplifications are generally introduced through the basic first order assumption or otherwise complexity is avoided through empirical means. Applicability of these methods are not questioned but the equations are concerned mainly with idealised performance of transport aircraft as opposed to the reality of various operational criteria. Issues of minimum control speed

*Senior Research Scientist.

Formerly employed by Saab Aircraft AB.
Graduate Member RAeS.

limited field performance, speed schedule formulation for climb, cruise and descent modes, fixed sector mission performance and associated optimal cost and profit flight techniques are not generally addressed. Studies have shown that the predictive powers of these methods display reasonable accuracy but objective function sensitivity to a generalised array of design parameters is left wanting when the notion of operational criteria are incorporated into the process.

Attempts have been made through the introduction of complex computer algorithms and multivariate optimisation (MVO) techniques like Quadratic Sequential Programming, Latin Squares, Decomposition, etc. in conjunction with calculus of variations and finite element theory, but unfortunately rather than truly achieving the goal of creating a market orientated competitive design, the sole end becomes an optimised mathematical model with no real reflection placed upon realistic operational concerns.

The purpose of this paper is to consider a middle ground between generalistic first order minimalism and more complex higher order MVO with emphasis still placed on simplicity but not at the expense of objective functionality and operational applicability. A number of revised as well as a variety of new methods are presented for calculation and subsequent design optimisation. These are validated against known aircraft designs as well as demonstrated with an actual small turbofan regional transport example.

Conceptual Design Prediction Methods

Concept of An Impulse Function

A traditional conceptual study revolves around analysis that is predominately discrete in nature. This can become quite cumbersome and impractical especially when typical conceptual design performance assessments even at the most elementary level can consist of hundreds or even thousands of point calculations, each requiring an instantaneous estimate. Additionally, this philosophy denies the possibility of conducting analytical performance optima identification via single expression algorithms, thereby in an effort to reduce complexity, it compels the use of coarser numerical integration procedures or closed form approximations prone to large

errors.

By introducing the concept of an impulse function or approximate unit step, normally discrete procedures of analysis can be transformed into continuous differentiable equations. The impulse function is mathematically approximated here as

$$\Phi(f, f_s) = k_1 + k_2 \tanh\left[k_3 \cdot (f - f_s)\right] \quad (1)$$

where the coefficients k_n represent values which assist in modelling an idealised unit step, and, the variables f and f_s are the tested and critical values respectively. For example $\Phi(10,20)$ results in 0 or conversely $\Phi(20,10)$ is 1. This idea can be extended for identification of maxima or minima between quantities as well. A maximising function can be produced via the associative rule

$$\Phi_{\max}(a, b) = a\Phi(a, b) + b\Phi(b, a) \quad (2)$$

whereas, a minimising function is of the form

$$\Phi_{\min}(a, b) = a\Phi(b, a) + b\Phi(-b, -a) \quad (3)$$

for the tested values a and b .

Atmospheric Modelling

It has been demonstrated⁽¹⁵⁾ temperature decreases linearly with altitude while the atmospheric hydrostatic relation equates density ratio lapse as some exponential function of temperature ratio. These relations hold true up to the troposphere, and when surpassed, temperature remains approximately constant with increasing flight level up to about 70000 ft or the lower part of the stratosphere. This altitude can be considered as an upper threshold of flight level well in excess of those frequented by contemporary subsonic transport aircraft. By incorporating an impulse function to mimic commencement of the tropopause [$\Phi_{trop} = \Phi(h, FL\ 361)$], the lapse rates for temperature (θ) and density (σ) ratio as a function of flight level (h) and International Standard Atmosphere temperature deviation (ΔISA) can be adequately modelled via

$$\theta = 1 + \frac{\kappa \Phi_{trop} (k_1^\theta h + k_2^\theta) + k_3^\theta \Delta ISA - h}{\kappa} \quad [FL\ 0, FL\ 700] \quad (4)$$

and

$$\sigma = \frac{\theta_{ISA} \sigma_{ISA}}{\theta} \quad [FL\ 0, FL\ 700] \quad (5)$$

where

$$\sigma_{ISA} = \theta_{ISA}^{4.2561} + \Phi_{trop} (k_1^\sigma \ln h + k_2^\sigma) \quad [FL\ 0, FL\ 700] \quad (6)$$

For instance, the coefficients $k_1^\theta = 6.900 \times 10^{-4}$ per FL, $k_2^\theta = -0.2480$, $k_3^\theta = 5.046$ FL^oC, $k_1^\sigma = -0.4398$, $k_2^\sigma = 2.583$ and $\kappa = 1454$ per FL would be used in order to model the atmosphere for given temperature deviation from ISA.

Another physical quantity important for the calculation of Reynolds number used for drag prediction is the ratio of sonic velocity to kinematic viscosity (a/ν) at given flight

level. Investigations have shown adequate results can be obtained via a third order polynomial curve fit.

Aircraft Weight Estimation

Constituent weight estimation is based on statistical fits of current production aircraft, and together with estimates for useful load, the sum of these constitutes the aircraft Maximum TakeOff Weight (MTOW). As is the case with most weight prediction methods in literature^(18,24), more refined estimates based on statistical equations through sophisticated regression analysis become transcendental algorithms characterised by relatively small and partially self cancelling errors with accuracies of the order of 5-10%. Studies showed this to be somewhat true for specific methods but were found to be wanting in many instances when adequate objective function sensitivity for rather advanced trade studies are desired. The final weight estimation algorithm adopted by the author involves a hybrid transcendental approach with Linnell's⁽¹⁴⁾ parametric description used for major components in conjunction with additional methods requiring fidelity from more specific parameters related to performance and geometry. By adopting Scott and Nguyen's⁽²⁰⁾ notion of two functional weight groups, a basis can be laid for derivation of the aircraft Operational Empty Weight (OEW). Since the sum of fuel and payload or useful load can be regarded as both a variable to optimise and the objective function, a third functional weight group is now introduced - leading to a combination of all three for MTOW.

The first functional weight group comprises of fuselage, wing, empennage and landing gear constituents and are derived via trend equations produced by Linnell. An adequate parametric representation of the relationship between applied loads, geometric shape and configuration choice was achieved with modifications made by the author to most of the trend coefficients. Since Linnell had allowed for an objective function sensitivity of dynamic pressure to structure, a direct coupling between fuselage structural weight and a design candidate's speed envelope or primarily v_{mo} speed were incorporated and together with the introduction of a limit manoeuvre-gust load parameter concept proposed by the author, this is envisaged to possess a consistent objective function sensitivity to a wide scope of the design parameters.

The second functional group designated as fixed equipment weight are estimated using a variation of the method given by Scott-Nguyen. The fixed weight is referred by Scott-Nguyen to be a "constant weight" because it is assumed to be related to passenger capacity and hence constant during the conceptual sizing process. The variation of a linear constant weight coefficient models the impact of fuselage size to fixed equipment and it can be quickly surmised that this parameter is specific to each respective manufacturer. The powerplant and installation weight including contributions made by nacelles and pylons is based on a logarithmic statistical regression produced by the author. The sample

size covered 66 different gas turbine engines produced by 7 manufacturers and each varying in maximum sea level static thrust capability between 8.5 kN (1900 lb.f) to 118 kN (26500 lb.f).

The third and final function group consists of weights characterised by ancillary geometric and philosophical considerations. These encapsulate estimation of available fuel weight with or without a center tank, and, contingency design maximum payload-OEW allowances. Maximum available fuel weight estimation was developed from a statistical correlation to wing geometry presented by Torenbeek⁽²⁴⁾ but was later modified by the author to reflect more contemporary data. Further algebraic extensions to this basic model were incorporated in order to facilitate more realistic fuel increments produced by introduction of a centre tank - this was considered important since many vehicles are frequently offered as standard or extended range versions. A philosophical decision of artificially increasing the desired maximum payload by some factor to create a contingency buffer for unexpected OEW penalties incurred during preliminary design is often considered in practise and is therefore also facilitated. To round off this functional group, an advanced technology multiplier to account for weight reduction possibilities of aircraft empty weight is also available. This parameter first proposed by Scott and Nguyen represents the progress of weight reduction over the last four decades with emphasis placed on vehicles with an average entry-into-service year (YEIS) of 1975.

Powerplant Installation

The attributes of a gas turbine powerplant are primarily dependent upon the effect of pressure ratio, altitude and free-stream velocity. The instantaneous production of thrust relies generally upon an engine's thermal efficiency in conjunction with variations in disc loading. The compression ratio is achieved partly by the inlet (ram pressure) generated by elevated mass flow at increased velocities but mostly through the compressor itself thus making pressure ratio engine specific. In view of this, an approximate engine model proportional to variation of flight level (h) and velocity (v) would be expected to generate an adequate description of thrust lapse.

By assuming this lapse rate decays exponentially, an approximation of instantaneous thrust can be proposed as

$$T = T_{oi} \left(1 + e^{-k_1 - k_2 h} T_o \right) k_3 e^{-k_4 h - k_5 v \exp[-k_6 h]} \quad (7)$$

where T is the instantaneous available thrust, T_{oi} is the installed maximum sea level static thrust and k_n are constants of proportionality. Eqn 7 is applicable for normal takeoff, maximum takeoff with auxiliary power reserve (APR), maximum climb and maximum continuous thrust ratings. A distinct maximum cruise thrust prediction method was also developed and is of the form

$$T = T_{oi} \left(1 + e^{-k_1 + k_2 h} T_o \right) k_3 e^{-\left(k_4 h + v \left[k_5 + k_6 \exp(-k_7 h) \cos\left(\frac{\pi}{4} + k_8 h\right) \right] \right)} \quad (8)$$

It can be observed that incorporation of an engine rating parameter for universal modelling which accommodates both takeoff/climb and maximum cruise has been dispensed with. Takeoff/climb ratings are usually associated with lower vehicular subsonic speeds whereas maximum cruise with considerably higher ones, and because present day gas turbine overall powerplant efficiencies exhibit strong variation with Mach number particularly in the transonic regime⁽²²⁾ i.e. Mach numbers greater than approximately 0.65, this condition denies adequate regression qualities - and therefore compels distinction from one another. Furthermore Eqn 8 need not be in an easily differentiable form for steady cruise analysis whereas as it will be demonstrated later Eqn 7 must.

Thrust specific fuel consumption (TSFC or c) is also a function of overall powerplant efficiency⁽²²⁾ and Mach number. Scope was given for the creation of a unified analytical treatment of instantaneous TSFC prediction so a single expression which accounts for not only Mach number but variations in engine ratings was pursued.

$$c = \left\{ k_1 h^{-k_2} \left(\frac{T}{T_{oi}} \right)^{(k_3 h + k_4)} \right\} M + (k_5 h + k_6) \left(\frac{T}{T_{oi}} \right) + k_7 h + k_8 \quad (9)$$

A linear performance deterioration model (k_θ) to account for the effects of temperature deviations from ISA (T_d) when calculating instantaneous available thrust or even TSFC may be incorporated via

$$k_\theta = 1 \pm k_1 \Phi(T_d, T_c) \quad (10)$$

where T_c is the critical ISA deviation for flat rating.

These expressions do not permit direct sensitivities to bypass ratio, pressure ratio or turbine entry temperature because such a facility was deemed too detailed for this level of analysis. Investigations have shown that adequate representation of these parameters are produced through correlation of lapse coefficients to the maximum static thrust rating of a given engine. In this way generic turboprop and turbojet models can be created through regression thereby giving good representation of expected overall powerplant efficiency without altering the inherent structure of the model itself. Due to the structure of the instantaneous thrust and TSFC models, they offer the opportunity of delivering relatively accurate predictions of thrust and fuel flow when a statistical regression for specific powerplants are done, and additional consideration to temperature deviations from ISA standard atmosphere and bleed losses can be incorporated when desired. If available, Reynolds number variation and other installation effects may be introduced thus allowing for accurate prediction, otherwise a generic model would possess the inherent capability of being utilised as a rubber engine for comprehensive sensitivity studies. Also, these functional forms are differentiable via logarithmic differentiation with respect to independent parameters which have a direct physical consequence i.e. flight level

and velocity, thus allowing for a rather comprehensive scope of performance optimisation possibilities.

Low-Speed and Enroute Aerodynamic Modelling

Lift Prediction

The clean wing maximum lift is derived from an algorithm developed by the author^(12,13) with a source database constructed utilising MIT's TODOR Vortex-Lattice software for a gamut of typical transport aircraft aspect ratio, taper ratio, root chord incidence and dihedral. Each generic planform was subsequently modified for a desirable lift distribution through wing tip wash out. High lift produced by flap and slat deflection are estimated based on methods presented by Young⁽²⁵⁾. This reference uses empirical correlation from assorted accumulated data and predicts with reasonable accuracy the aerodynamic characteristics of high lift devices. Combined with a wide variety of device choice for estimation this was found to be most suitable.

The final combined method accounts for effects due only to wing aspect ratio, taper ratio as well as quarter chord sweep and does not consider wing section thickness and camber in an effort to reduce complexity. Abbott and Von Doenhoff⁽¹⁾ show that for the interval of mean wing thicknesses commonly employed for modern day transport aircraft, the variation of sectional maximum lift characteristics is generally small except for thickness ratios less than 12 percent and the effects of increasing camber to wing section increased lift becomes less significant for thicknesses greater than 12 percent. Additionally, scale effects due to Reynolds number for thickness ratios between 12 to 24 percent were experimentally found to be nearly independent of thickness ratio. It is felt that wing geometry trades via mean wing section thickness would be more influential in terms of structural efficiency, available fuel capacity and enroute compressibility drag rather than drastically alter for example field performance by a small incremental change in lift.

Low-Speed and Enroute Drag Prediction

When formulating predicted drag polars at the conceptual level, it is common practise to neglect variations in Reynolds number and centre of gravity location reducing the analysis to a narrow band of what is considered as the typical scenario. This approach suffers from great inconsistencies when variations in drag occurs with Mach number at low subsonic speeds or in particular when compressibility effects become significant. After careful review of the impact each simplification has to the final result, a different approach to drag estimation was created by the author which introduces the influence of Reynolds number but retains the previous assumption of negligible contributions due to center of gravity. The goal was to establish a single algorithm (CDM) which covers the entire spectrum of operation for transport aircraft whilst still maintaining a good degree of accuracy. Furthermore,

an additional stipulation of differentiability for subsequent performance optimisation purposes was also pursued.

Vortex-induced drag estimation for field and enroute regimes together with other sources such as profile drag increments from flap deflection, roughness, excrescences, interference and three dimensional effects are treated by traditional empirical models^(17,18,24) but have been adjusted where required.

A common method for determining the zero-lift drag of aircraft components is an assumption that the constituent's friction drag is equivalent to a flat plate having the same wetted area and characteristic length. In this way, the preliminary stage of a complete vehicular zero-lift drag estimation may be accomplished by summation of these individual components. By creating a hybrid approach where the component build-up method is benchmarked against a standardised closed form expression, economy of effort can be achieved without incurring excessive degradation in predictive powers.

A tool for estimating zero-lift drag (C_{Do}) is the friction coefficient equation based on experimentation done by Eckert⁽⁴⁾ which accounts for fully turbulent flow and compressibility effects. By assuming an appropriate reference condition of Mach number and flight level, the component build-up method may be employed and a characteristic equivalent length (l_e) for the entire vehicle can be derived from its equivalent skin friction coefficient - a quantity commonly used for aircraft comparison exercises. This equivalent characteristic length may in turn be reintroduced into Eckert's Equation and solved for any other Mach number (M) and flight level (h) combinations the aeroplane encounters, viz.,

$$C_{Do}|_{M,h} \cong \frac{A \{ \ln[10] \}^b}{\left[\ln \left\{ M l_e \left(\frac{a}{\nu} \right) \right\} \right]^b \left[1 + c M^2 \right]^d} S_{wet} \quad (11)$$

where a represents the sonic velocity at flight level, ν the kinematic viscosity at flight level, S_{wet} is the total wetted area of the vehicle and constants A , b , c and d are coefficients of proportionality derived by Eckert.

In an effort to theoretically gauge the magnitude of inherent errors produced by this approach, the equivalent characteristic length method (ECLM) expression was reconfigured as an error function and resultant equivalent skin friction errors were observed for a range of contemporary regional transport and business jet Reynolds number regimes. For a typical enroute Reynolds number of 1.5×10^6 based on vehicular characteristic length, errors of -27% in the equivalent characteristic length correspond to a +5% overestimation of equivalent skin friction or total zero-lift drag. Conversely, for the same Reynolds number, a -5% underestimation of zero-lift drag is tolerated by a +33% error in equivalent characteristic length. This result shows the resilience of ECLM.

Compressibility effects on drag are commonly described by arbitrary mathematical models because much of what is known about the mixed flow regime is largely experi-

mental. At the conceptual level they generally do not adequately account for the dependence of drag divergence Mach number on design parameters like instantaneous lift coefficient, wing sweep, mean wing thickness and type of airfoil geometry but are estimated with simple empirical increments. As an alternative, Torenbeek⁽²³⁾ offers a variation of Korn's Equation⁽²⁾ to quantify the limits of wing section performance. After some manipulation⁽¹²⁾ of the modified Korn's Equation, the critical Mach number (M_{cr}) can be estimated as

$$M_{cr} = \left\{ \frac{1}{\cos \Lambda} \left[M_{ref} - \frac{1}{10} \left(\frac{C_L}{\cos^2 \Lambda} \right)^{3/2} - \left(\frac{t/c}{\cos \Lambda} \right) \right] \right\} - \Delta M \quad (12)$$

where Λ is the wing quarter chord sweep, C_L the instantaneous lift produced by the wing, t/c is the mean wing thickness ratio, M_{ref} is an empirical wing section technology factor and ΔM is an empirical representation of the relationship between M_{cr} and divergence Mach number (M_{DD}). In order to produce a continuous function concept for compressibility drag (ΔC_{Dcomp}), the critical Mach number threshold can be flagged by an approximate impulse function [$\Phi_{Mcr} = \Phi(M, M_{cr})$] and combining this with an empirical drag rise model given by Torenbeek⁽²⁴⁾ this yields

$$\Delta C_{Dcomp} = \Phi_{Mcr} \Delta C_{DD} \left[1 + \Phi_{Mcr} \left(\frac{M - M_{cr}}{\Delta M} - 1 \right) \right]^n \quad (13)$$

thus making the expression differentiable for all Mach numbers.

The one engine inoperative (OEI) condition appears to be mostly disregarded in conceptual design literature. It is usually classified as a preliminary design problem^(18,24) because yawing and rolling considerations become rather complex in nature since these must be trimmed out by primarily the rudder and then aileron. Drag due to engine windmilling, airframe sideslip, incremental changes in normal force induced and profile drag from control surface deflection, asymmetric slipstream effects and lift distribution reconfiguration producing vortex-induced contributions all combine to complicate matters. By examining the exact approach, a number of valid simplifications may be incorporated in order to reduce the scope of detailed information required whilst retaining strong predictive powers and objective function sensitivity with respect to the design variables.

Studies have shown that many of these constituent contributors can be neglected with the exception of induced and profile drag generated by rudder deflection. Figure 1 demonstrates the pertinent forces and moments once this simplification is introduced. It is assumed that the vertical tail utilises a symmetric profile and all rudder deflections during asymmetric flight will be below stall, thus, from linear thin aerofoil theory, the rudder deflection (δ_r) required for equilibrium of the OEI asymmetric condition is given by

$$\delta_r = \frac{2 y_{eng} (D_{wm} + T_{op})}{\rho v^2 S_{vt} C_{L\alpha} \tau \eta l_{vt}} \quad (14)$$

where y_{eng} is the moment arm from fuselage center line (assumed centre of gravity location) to the critical and wind-milling engines, D_{wm} is the drag produced by the wind-milling engine and is estimated using empirical methods, T_{op} is the instantaneous available thrust produced by the critical engine at velocity v , S_{vt} is the vertical tail reference area, $C_{L\alpha}$ is the lift-curve slope characteristic of the vertical tail, τ is the flap effectiveness factor, η is a correction which accounts for the effects of viscosity and l_{vt} is the vertical tail moment arm. It is highlighted that $C_{L\alpha}$ estimates are adjusted for aspect ratio with the Hemboltz Equation⁽¹⁵⁾ and effects of sweep by a first order cosine relation⁽²⁴⁾. From this basis, the possibility of accounting for the influence of minimum control speed limitations on field length and climb performance can be introduced at the conceptual level, and, the method for predicting this aspect of operational performance is discussed with greater detail in the section to follow.

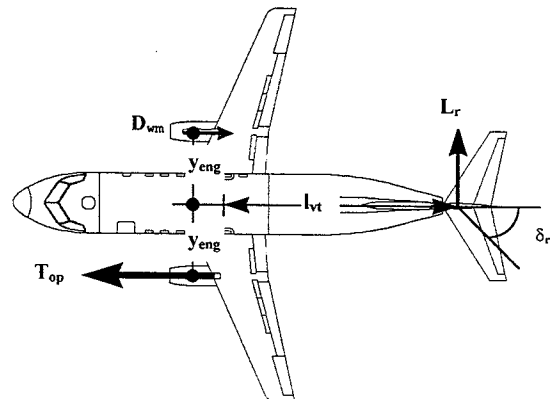


FIGURE 1 - Simplifications of forces and geometric considerations during the asymmetric thrust condition.

By summing the forces and moments in Figure 1 and quantifying rudder deflection from Eqn 14, the incremental drag contribution produced by OEI asymmetric condition (ΔC_{DOEI}) is therefore given by

$$\Delta C_{DOEI} = \frac{2 \left[D_{wm} + (D_{wm} + T_{op}) \frac{y_{eng}}{l_{vt}} \tan \delta_r \right]}{\rho v^2 S_{vt}} \quad (15)$$

This relation is not only applicable for low speed field performance drag prediction, but can also be utilised for climb out analysis as well: specifically in relation to OEI maximum attainable flight level and driftdown proficiency trade studies at ISA and more importantly off-ISA conditions.

Field Performance

Takeoff and landing field length prediction can become quite complex if one approaches the problem via integral methods. Many alternatives for the estimation of field

performance exists in current literature. Rather than opt for new algorithms, existing methods found in literature were utilised but with some enhancements introduced by the author.

Torenbeek⁽²⁴⁾ offers a useful equation in functional form which correlates the field length performance of similar aircraft and this serves as an adequate first order approximation.

$$BFL = \left(\frac{0.863}{1 + 2.3 \Delta\gamma_2} \right) \left(\frac{W_{to}/S_w}{\rho g C_{L_2}} + h_{to} \right) \left(\frac{1}{T/W_{to} - \mu'} + 2.7 \right) + \frac{\Delta s_{to}}{\sqrt{\sigma}} \quad (16)$$

where $\gamma_2 = T/W - C_D/C_L$ is the instantaneous OEI climb gradient of the vehicle at the 35 ft (10.7 m) screen height threshold (h_{to}), $\Delta\gamma_2$ is γ_2 less the minimum second segment climb gradient permitted by airworthiness authorities, W_{to}/S_w is the wing loading at TakeOff Gross Weight (TOGW), T/W_{to} is mean thrust-weight for the takeoff run, C_{L_2} is the instantaneous lift coefficient at v_2 speed, μ' is the coefficient of friction during acceleration and Δs_{to} is the inertia distance. The asymmetric drag-lift ratio is calculated based on the most limiting condition when taking the stall speed factored (v_2/v_s) and the minimum control (v_{mc}) speeds into consideration. The v_{mc} can be derived by rearranging Eqn 14 and solving for an instantaneous velocity when maximum permissible rudder deflection occurs (i.e. $\delta = \delta_{max}$) - the resultant transcendental equation thereby deriving minimum control speed on the ground which is also treated as an approximation of minimum control speed in the air. In this way, an objective function sensitivity with engine thrust line location as well as thrust generation potential to balanced field length performance can be established and hence locate any stationary point thresholds.

The landing segment can be separated into three portions of operation: approach, flare and the ground roll. The method presented by McCormick⁽¹⁵⁾ offers an opportunity of not only producing reliable predictions but is comprehensive enough for adequate objective function sensitivity. The flare is assumed to be a circular arc and approach speed is constant throughout the flare. After touchdown, delay time allowances are made for reconfiguring the vehicle from landing to braking, and finally, the ground roll is simply defined as a continuous deceleration where upon the magnitudes of all relevant variables are evaluated at the root mean square of touchdown speed. Approach and landing climb minimum control speed thresholds have been disregarded in this instance since these scenarios are usually not limiting at ISA, s.l. conditions although exceptions may occur where positive engine thrust levels are significant in some vehicles.

The coefficient of friction for acceleration and braking is estimated using linear fits with drag-lift ratio (takeoff) and root mean square touchdown speed (landing) respectively. Additional refinements through introduction of spoiler actuation and thrust reversing capability modelled by

empirical methods are also available to enable regulatory flexibility (JAR or FAR) as well as demonstrate performance improvement possibilities.

Enroute Performance Assessment

Operational Limitations

Appropriate formulation of the flight envelope is essential for maximising the enroute performance capabilities of any respective aircraft and many regulatory guidelines exist for its definition⁽²⁴⁾. The problem here is to create a set of simplistic rules which allows for accurate envelope construction without unduly restricting the vehicle's unconstrained predicted performance. The flight envelope usually consists of four distinct boundaries, three of which are defined by placard speed thresholds related to stall (v_s), buffeting and emergency dive (M_{mo}), and, a combined consideration of manoeuvre-gust loads and maximum dynamic pressure (v_{mo}). The remaining boundary is an upper threshold of flight level derived from simultaneous appreciation of climb thrust limitations, maximum cabin pressure differential and occasionally buffeting. The derivation of these boundaries are commonly performed using extrapolated wind tunnel data to full-scale and subsequently verified with flight testing. Initial prediction methods can become mathematically quite extensive which do not easily lend themselves to simplification or otherwise lose significant precision in the process. For example buffeting is characterised by breaks in $C_L-\alpha$, $c_m-\alpha$ or $c_x-\alpha$ curves and emergence of pressure divergence on any of the lifting surfaces or fuselage - this poses a daunting challenge from the analytical point of view. By tackling this problem through the basic conceptual design philosophy of implicit minimum goal success, a useful empirical method may be developed that adequately defines the flight envelope without the need for more esoteric aerodynamic modelling. This approach uses the information already available from an investigated vehicle's unconstrained predicted performance and correlates this to a database of previous observations collected from known designs.

Initially, the stall speed placard is trivially calculated as an aerodynamic minimum speed with power off. The upper flight level boundary can be derived from known climbing performance of the vehicle with some attention paid to performance and structural limits - this matter is clarified further in the section to follow. By assuming that buffet onset and minimum buffet margin violation can be avoided, the maximum projected service ceiling for certification can then be predicted. The v_{mo} and M_{mo} placard speeds are set using known maximum cruise thrust limited performance for a predesignated minimum flight weight (MFLW) vehicle configuration with adjustments incorporated from statistical bias. The MFLW can be defined by assuming some percentage of the vehicle's MTOW: this figure may be obtained from comparisons made with Performance Engineer Handbooks (PEH) of other known designs or equivalently estimated by assuming an All-Up Weight (AUW) equal to the sum of

OEW and 25% of the Maximum Fuel Weight (MFW). Thereafter, the maximum cruise speed threshold can be obtained assuming equilibrium of forces in horizontal flight for given MFLW at a specified interval of flight levels commonly assumed to be between FL 150 and FL 300 in order to maximise enroute performance flexibility. This speed variation with flight level is in fact hyperbolic, however using the same reasoning for Eqn 19, a transformation of speed as an exponential function of flight level can be introduced and appropriate placard speeds can then be predicted based on statistical regression from a database derived from other aircraft.

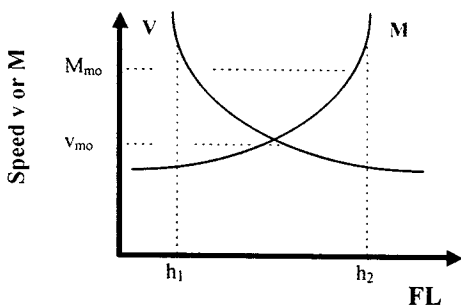


FIGURE 2 - Identification of v_{m0}/M_{m0} flight envelope boundary using "20-80" rule.

For example if a design proposal is to be inspected for its predicted v_{m0}/M_{m0} boundaries, maximum cruise speed (v_{mcr}) for flight levels h_1 and h_2 assuming MFLW are investigated, and correspondingly plotted as free variables of calibrated air speed (CAS) and Mach, thus a cross plot similar in form to Figure 2 can be established. It is evident that Mach number tends to increase with increasing flight level whereas CAS increases with reduction in flight level. By considering these curves as potential M_{m0} and v_{m0} candidates respectively and introducing the "20-80" rule, the vehicle's v_{m0}/M_{m0} boundary can be predicted. The 20-80 rule is actually an interval which excludes 20% of the slower CAS and faster Mach speed portions of the investigated flight level interval and was derived empirically. One drawback is that the method does not facilitate a multiple v_{m0}/M_{m0} boundary definition, however the approach is simple, promotes synergistic utilisation of primary conceptual calculation algorithms and validation has shown it to be relatively accurate.

Climb and Descent Control Formulation

Neglecting flight path-angle dynamics and effects of wind, the point mass equation of motion for accelerated flight in the vertical plane is

$$\frac{dh}{dt} = \frac{(T-D)v}{\left[1 + \frac{v}{g} \frac{dv}{dh}\right]W} \quad (17)$$

where dh/dt is the instantaneous climb rate, T , D , and W are instantaneous available thrust, total drag and AUW at

forward velocity v , and the final component accounts for accelerated climbs. Operational conventions dictate a definition of flight level which gives reasonable measure of maximum operating height potential for an aircraft whilst simultaneously fulfilling legitimate considerations of attaining this height in reasonable time. A well tempered conceptual climb control formulation for any prospective aircraft should therefore weigh the attributes of maximum rate of climb (ROC) and minimum time to climb optimal trajectories and create a final approximate trajectory which would be used for the definition of a maximum service ceiling or flight envelope upper threshold. Since ROC is proportional to specific excess power, satisfying the condition

$$\frac{\partial[(T-D)v]}{\partial v} = 0 \quad (18)$$

and subsequently rearranging as a transcendental function would allow identification of optimal instantaneous forward speeds at given flight level and AUW since available thrust and total drag have been previously defined as continuous differentiable functions. If speed profile is plotted as an optimal climb trajectory is generated, the resultant locus shows strong hyperbolic tendencies with flight level. This circumstance unfortunately requires an integral approach or its common approximate numerical alternative. Conversely, if flight level can be regarded as a free variable against optimal forward speed, it is evident that this transformation promotes an approximate exponential progression to mimic the profile. Consequently, if two reference flight levels can be selected which minimise the error incurred when weight loss due to fuel burn is neglected, i.e. rate change of speed with respect to flight level does not vary greatly between each reference flight level, an adequate approximation for the locus of forward speed for an optimal climb trajectory covering the entire flight level envelope can be constructed. For example, at reference flight levels h_1 and h_2 , the corresponding instantaneous forward speeds v_{h1} and v_{h2} can be expressed as

$$v_{h_1} = k_1 e^{k_2 h_1} \quad \text{and} \quad v_{h_2} = k_3 e^{k_4 h_2} \quad (19)$$

and after solving these simultaneous equations for constants of proportionality k_n , a single closed form expression can approximate an optimal climb trajectory forward speed at given flight level. A conceptual service ceiling estimate would require two distinct profiles based on the premises of idealised acceleration-free and accelerated climb scenarios in order to derive a realistic optimal accelerated climb trajectory. A splay resulting from these distinct schedules are then constructed and subsequently compared for a resultant closer approximation to the actual accelerated climb profile. The original accelerated climb is initially approximated via an analytical approach which traces a path of speed loci where lines of constant height-energy are tangential to curves of specific excess power. However, this procedure

is not sufficient enough for final optimal trajectory definition because it assumes that potential and kinetic energy can be interchanged instantaneously and without loss thereby yielding speed schedules with optimistically higher velocities. The final speed profile constitutes a predicted vehicular maximum service ceiling but is only regarded as an upper limit the vehicle is capable of fulfilling. This in turn does not necessarily constitute the aeroplane's final service ceiling because other considerations of operational flexibility and structural limitations which are mostly based on an intuitive trade must be taken into consideration.

It is common practise to assign two distinct climb modes or more specifically speed schedules for climb control by means of fixed CAS and Mach speeds. The advantages with faster speed schedules are that they create possibilities in conducting further time, cost or profit function optimisation, or more importantly opportunities in constraining previously unconstrained optima compared to single speed schedules because faster climb speed schedules (designated here as CLB Mode H) encourage cruise "soaking"⁽¹²⁾ or the exchange of cruise distance for climb which leads to significant block time reductions - this especially being the case for regional type sector missions. Furthermore, a slower climb speed schedule (CLB Mode L) enables closer adherence to fuel optimal procedures during climb thereby enhancing range capability. In this way, CLB Mode L and CLB Mode H speed schedule definitions are formulated with respect to optimal climb trajectory profile state and time function adherence and designated divergence criteria respectively.

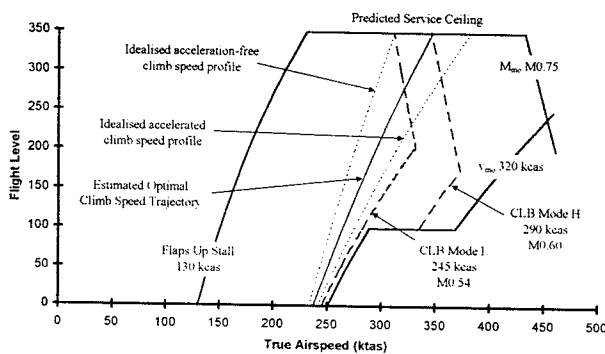


FIGURE 3 - Example optimal climb trajectory, climb control speed schedule and flight envelope definitions.

It is common practise to neglect weight loss due to fuel burn, however, the effect of weight loss on trajectory becomes important in two respects: a greater degree of operational flexibility through higher ceiling capability may be afforded if an optimal trajectory for block time, cost or profit functions are denied i.e. air-traffic control (ATC) or route structure, and, greater scope for improvements in efficiency of fuel load burned for range can be achieved or at least traded for feasibility. By introducing a fuel burn model via exponential extrapolation, not only can better approximations for

actual time, distance and fuel burn be modelled as the trajectory is generated for given speed schedule from an initial TOGW, but occasionally, valid predicted performance enhancements may be exploited.

Descent speed schedule definitions are mostly treated in the same way as climb with CAS, permissible vehicular as well as cabin maximum rate of descent (ROD) as the control variables. In this instance multiple descent modes are disregarded in favour of one DES Mode owing to small differences in the state and time variables.

Optimal Cruise Control Identification

The objective here is to derive a single expression to instantaneously derive optimal cruise conditions at constant flight level. For an accurate assessment of maximum specific range (SAR), optimisation should focus on the control variables of speed, flight level and overall powerplant efficiency⁽²²⁾. At the conceptual level it is customary however to introduce a critical assumption that thrust specific fuel consumption is independent of throttle setting together with large variations in Mach number for the sake of simplicity. Since the structure of the thrust specific fuel consumption model presented earlier facilitates these dependencies, a single expression algorithm can be formulated to identify the condition for optimal cruise performance.

The need for throttle setting (T/T_o) can be determined a priori and incorporated in the following manner

$$\frac{\partial(T/T_o)}{\partial v} \equiv \frac{\partial(D/T_o)}{\partial v} \equiv \frac{1}{T_o} \frac{\partial D}{\partial v} \quad (20)$$

where the total drag D consists of zero-lift, induced and compressibility contributions and hence dispensing with the need for a partial power thrust model. By employing Miller's⁽¹⁶⁾ logarithmic differentiation of the Breguet equation with respect to speed and introducing the additional control variable of throttle setting, the generalised criteria for maximum specific range speed (v_{opt}) at flight level h is given by

$$v_{opt} = \frac{1}{\frac{1}{c} \left(\frac{\partial c}{\partial M} \right)_h \left(\frac{\partial M}{\partial v} \right)_h + \left[\frac{1}{c T_o} \left(\frac{\partial c}{\partial [T/T_o]} \right)_h + \frac{1}{D} \right] \left(\frac{\partial D}{\partial v} \right)_h} \quad (21)$$

where c is the thrust specific fuel consumption. It can be observed that this transcendental expression is comprehensive enough to offer a thorough treatment of identifying not only partial and global cruise performance optima but has the flexibility of finding such solutions below the drag rise and more importantly identification of optima within the transonic regime as well. In order to inspect for consistency of these unconstrained solutions against operational limitations, comparison to the thrust limited speed, maximum operating limit speed and maximum operating limit Mach number at flight level are also considered via a minimising function, viz.

$$v_h^* = \Phi_{\min} \left[\Phi_{\min}(v_{opt}, v_{mcr}), \Phi_{\min}(v_{mo}, M_{mo}) \right] \quad (22)$$

where the maximum cruise speed threshold at flight level is simply obtained assuming equilibrium of forces in horizontal flight.

Enroute Operational Performance and Flight Profile Optimisation

The optimum trajectory-profile algorithm (OTPA) analyses a three-phase flight in which interactions between climb, steady cruise and descent are considered in order to allow for inspection of objective function sensitivities against the collective influence imposed by a general set of design variables. Rather than attempt to approach this problem via a fully blown calculus of variations⁽⁷⁾ or even its simplified version⁽²¹⁾, the idea was to create algebraic functions which can adequately describe the constituent known trajectories, thence combine all segments in order to construct an assumed trajectory and optimise for any state or time function. Cost and subsequent profitability functions together with their inherent sub-optimisation possibilities are also considered but are presented in the next section of this paper.

During climb and descent it customary to correlate distance travelled, time elapsed and fuel expended as free variables against an instantaneous TOGW or AUW and flight level. A transformation using the assumption that AUW, time elapsed and fuel expended (all denoted by variable λ_h) are monotonic functions of distance travelled at a particular flight level (d_h) can be expressed as

$$d_h = e^{\left(\frac{\lambda_h - k_2}{k_1}\right)} \Leftrightarrow \lambda_h = k_1 \ln(d_h) + k_2 \quad (23)$$

An impulse function for Eqn 23's flight level dependent coefficients (k_n) give instantaneous values of otherwise free variables thereby enabling a solution for trajectory optimisation through known distance and flight level.

Steady cruise is conducted at constant flight level and depending on the accuracy desired the distance traversed may be numerically integrated as aircraft mass is reduced, however, experience has shown using Eqn 22 or maximum cruise speed at an average cruise AUW is sufficient enough for a good approximation. The possibility of examining intermediate CAS for steady cruise has been disregarded since these scenarios are perceived to be inconsequential with regards to a design proposal's operational and cost objective functionality. Instead, a choice of throttle setting limited to two particular procedures, i.e. maximum cruise power afforded by the thrust model previously presented in Eqn 8 and partial power setting (as per the rationale given in Eqn 20) required for optimal cruise performance, is given in order to facilitate optimal fuel usage (maximum SAR and minimum fuel), maximum block speed, optimal time expended (minimum time) and intermediate flight techniques for payload-range and block time-fuel curve characteristics.

OTPA begins with an initial flight level assumption of maximum service ceiling. For reasons of computational speed and simplicity, the algorithm utilises an interval halving numerical scheme with climb distance as the free variable - an upper and lower climb distance interval at flight level can be derived when MTOW and MFLW are assumed respectively. Based on this premise, other pertinent parameters such as the fuel expended to clear flight level, time elapsed to climb and TOGW are quantified for the interval mid-point. The first iteration assumes an initial beginning of descent (BOD) AUW to be the sum of OEW, payload and fixed fuel reserves which then permits an estimate of available fuel for cruise. The scheme then proceeds until satisfaction of either of the two conditions arises: (a) fuel weight balance occurs for payload-range, or, (b) distance balance occurs for fixed sector missions. Holding can be defined via a preselected minimum drag or fixed speed schedule for given flight level and time duration and is initially quantified from an AUW comprising of OEW, payload and diversion reserves. The diversion reserve is formulated using the iterative scheme discussed above but only considers a minimum fuel flight technique since fixed sector distances are usually considered. Further reserve contingencies may be accommodated through selection of an extended cruise time duration option as well as the possibility of assuming some fixed percentage of the total flight fuel. The algorithm facilitates inequality constraints of: a minimum cruise fraction to ensure cruise segments do not become too small and compromise passenger comfort; operational limitations imposed by structure, design weight thresholds and powerplant; and, any other aircraft model, ATC or route structure limitations that require consideration.

The introduction of an additional criterion whereby block speed is maximised promotes iteration to lower flight levels thus allowing for the identification of maximum block speed and minimum time flight techniques for payload-range and fixed sector mission respectively. A presentation with payload-range block speed maximised can be useful for objective function sensitivity studies where the designer may wish to trade the merits of a particular design candidate's maximum attainable sector mission stage length for given mission payload against other potential configurations or even compare results against known competitor aircraft performance. After intensive investigations it was decided that a pre-selected speed schedule combination for given distance, time and fuel variable optimisation would offer a tangible reduction in algorithm complexity without any undue compromises in accuracy. OTPA defines maximum block speed and minimum time flight techniques as procedures comprising of CLB Mode H, maximum cruise (MCR) and DES Mode at optimal flight level, whereas, the maximum SAR and minimum fuel flight techniques always assume CLB Mode L, maximum range cruise (MRC) and DES Mode conducted at service ceiling and do not undergo any flight level iterations unless inequality constraints such as a minimum cruise fraction violation require it to do so.

Direct Operating Cost, Return On Investment and Associated Optimal Flight Techniques

The effect of block speed (or time) variation results in markedly different block speeds when minimum fuel, minimum time, minimum direct operating cost (DOC) and maximum return on investment (ROI) are compared for fixed sector distances with given mission criteria. These concepts, in part or collectively depending on the role of the vehicle, are integral for gauging the merits of new conceptual designs since they quantify operational flexibility. Even if the problem is reduced to the first order level, non-linearities still predominate hence not affording the designer clues to what variables exert strong influences. Other options include the use of MVO algorithms which deny the designer control over the final trade consideration of optimal solution versus feasibility. The idea is to utilise a standardised array of models which are universally consistent and are empirically derived for each trade study investigated by the designer.

All operational aspects are considered in terms of potential objective functions that might exhibit dependence to flight technique. Indeed, the problem of speed schedule formulation with respect to optimal operational performance could even be considered here but is not generally dealt with in this phase of design: it is felt that such an investigation should belong to the realm of refined sizing such as the initial phases of preliminary design work or product operational performance improvement programmes for existing vehicles.

The merit of any given flight technique can be weighed from a proposal's block time-fuel curve summary. These curves represent for a given sector distance and mission criteria thresholds for minimum time as well as fuel, and, intermediate flight techniques yielding height-energy block fuel minima for fixed block times between these two extremes. Since the block time-fuel summary is made up of a collection of different predetermined speed schedules and flight techniques, i.e. distinct climb, cruise and descent modes at a specific flight level, the curve geometry is constructed through a combination of quasi-discrete and discrete points indicative of high and intermediate-low speed techniques. One may conclude that the block time-fuel summary is a complex function that can not be easily represented by an analytical expression coupled to a general set of aircraft parameters; in fact to achieve this goal the calculus of variations⁽⁷⁾ approach must be employed and this is unfortunately not a viable option for conceptual work. The failure of this option implies that another philosophy may be required: a model using hyperbolic functions appears well suited to the curve definition exercise and for a given sector mission is suggested here as

$$W_{fuel} = W_{f, \min time} (1 - k_1) \tanh \left[k_2 (t_{\min time} - t) \right] - W_{f, \min fuel} (1 - k_3) \tanh \left[k_4 (t_{\min fuel} - t) \right] + k_5 \quad (24)$$

where W_{fuel} is block fuel in the closed block time interval $[t_{\min time}, t_{\min fuel}]$, $W_{f, \min time}$ the block fuel for a minimum time flight technique, k_1 and k_2 constants which allow for the impact of different higher speed technique attributes to assorted combinations of intermediate schedules, $W_{f, \min fuel}$ the block fuel for a minimum fuel flight technique, k_3 and k_4 constants which allow for the impact of different lower speed technique attributes to assorted combinations of intermediate schedules, and k_5 is an arbitrary constant. Investigations have shown the non-linear coefficients in Eqn 24 can not be explicitly related to a specialised set of design variables or expressed as consistent continuous functions of variables like for example sector distance, but, this function is differentiable and more poignantly allows for the identification of optimal flight techniques. In order to facilitate the continuous function concept, two additional models are introduced. A maintenance/materiel cost model for the sample closed interval $[t_0, t_n]$

$$c_{main, thr} = c_{main} + \frac{\alpha_{main}}{(t - t_{man})^{\beta_{main}}} \quad (25)$$

where $c_{main, thr}$ is the total maintenance time dependent cost, c_{main} is the flight time dependent maintenance cost denoting theoretically most efficient work practise or learning curve asymptote, α_{main} and β_{main} are constants of proportionality, t_{man} is the manoeuvre allowance and t is block time. A yield model indicating a measure of ticket prices (Y_{sec}) with respect to stage length s is presented as

$$Y_{SEC} = y_1 \lambda PAX s \left(1 + y_2 \tanh \left[y_3 (s_{ref} - s) \right] \right) \quad (26)$$

where λ is passenger load factor for given sector mission, PAX is the maximum passenger capacity of the aircraft, s_{ref} is the reference stage length and y_n are constants of proportionality. Combined with the other standard cost methodologies available in literature^(10,11), identification of cost minima and profit maxima coupled to variation of flight technique or block time can be ensured.

For a given reference time frame utilisation, optimum flight techniques were found to be governed by the conditions

$$\begin{aligned} \frac{dC_{DOCS}}{dt} = 0 & \quad \text{Min. DOC, hourly and fixed} \\ & \quad \text{departures based utilisation} \\ \frac{dP}{dt} \equiv \frac{dC_{DOCS}}{dt} = 0 & \quad \text{Max. ROI assuming fixed departures} \\ & \quad \text{or} \\ \left(\frac{\partial P}{\partial N_s} \right)_s = 0 & \quad \text{Max. ROI, hourly based utilisation} \end{aligned} \quad (27)$$

where C_{DOCS} is the DOC per sector mission, N_s is the number of sectors completed per given reference time frame and P is the ROI per sector mission or time frame. Both DOC and ROI optimal flight techniques are categorised as constrained or unconstrained⁽¹¹⁾. The con-

strained condition denotes a flight technique yielding block times within the closed interval $[t_{\min \text{time}}, t_{\min \text{fuel}}]$, whereas, the unconstrained condition signifies a requirement of block times faster than the lower block time threshold physically permissible by a given vehicle. Pertinent conclusions drawn from this study concern the relationship of cost and profit optimal flight techniques to one another. An hourly based utilisation theoretically results in distinct flight technique optima for minimum cost and maximum ROI. The ROI optima are characterised by faster block speeds than cost optimal ones because of a co-dependence on block time and the quantity of aircraft seat-miles completed by the vehicle. A fixed number of sectors utilisation assumption reduces the sensitivity of time related costs to flight technique and thus minimise the significance of this component compared to the fuel expended. This situation produces block speed optima appreciably slower than those assuming an hourly based reference time frame utilisation. Furthermore, the fixed departures assumption theoretically creates a condition where both cost optimal and profit optimal flight techniques coincide with one another. Since an hourly based reference time frame utilisation results in partial ROI optima for specific sector distances, this implies the existence of a global optimum at some specific stage length and block time. An ROI model was developed in order to identify this condition. The model is proposed as

$$P = (\Phi_\alpha s - \Phi_\beta) e^{-(\Phi_\gamma + \Phi_\delta s)} + \Phi_\epsilon \quad (28)$$

between the lower and upper stage length thresholds of the surveyed interval $[s_o, s_n]$. Fortunately, this information can be exploited for ensuring profit earning flexibility for future transport aircraft design proposals. If the model given above is actually taken into consideration as an open interval, for example, $[s_{be}, \infty)$ or from break even stage length and upwards, one can identify uncanny similarities to a typical step response of stable linear control systems as exemplified by Figure 4. Subsequently, a collection of merit parameters which give rise to the ability of sub-

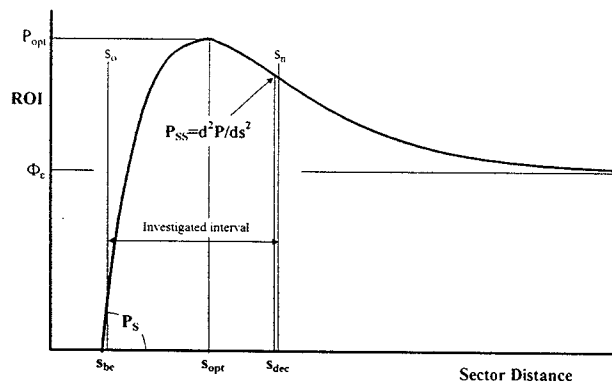


FIGURE 4 - Typical stage length response of ROI assuming an hourly based reference time frame utilisation.

optimising for more desirable ROI characteristics can be formulated from the model's own intrinsic behaviour.

Break even stage length (s_{be}) and corresponding pre-optimum ROI rise rate (P_s), the ROI global optimum (P_{opt}) and corresponding stage length (s_{opt}), the post-optimum ROI decay rate (P_{ss}) together with the magnitude of the model's asymptote value (Φ_ϵ) are suggested as a logical sequence of guidelines when conducting new conceptual aircraft designs or even detailed competitor reviews.

Prediction Method Effectiveness

In order to validate the methodology effectiveness and relative simplicity, a spreadsheet based software package called QCARD or Quick Conceptual Aircraft Research and Development was designed. A wide variety of known regional aircraft were input and QCARD's predictive powers were inspected against each respective vehicle's manufacturer PEH or its equivalent. The aircraft used for this validation exercise were: the 19 PAX PD340-2⁽¹³⁾; 37 PAX Embraer RJ135⁽⁵⁾; 50 PAX Saab 2000⁽¹⁹⁾, Embraer RJ145⁽⁶⁾ and Canadair RJ100⁽³⁾; 70 PAX Fokker 70⁽⁸⁾; and 100 PAX Fokker 100⁽⁹⁾ vehicles.

The known drag performance characteristics of the Saab 2000 were available to validate the predictive powers of CDM. Figure 5 shows the agreement between CDM calculations and the flight test drag polars - it can be discerned that a $\pm 5\%$ maximum error bandwidth was produced for Saab 2000's entire flight envelope. Although the overall drag polars produced by CDM show good

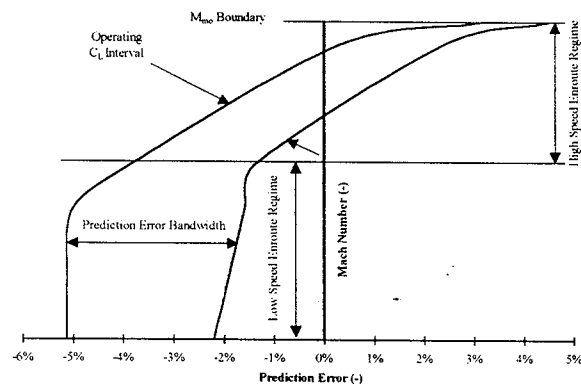


FIGURE 5 - CDM predictions against flight test drag polars for the Saab 2000, enroute configuration.

agreement to flight test data in the operational envelope, validation for objective function sensitivity of the drag constituents was not conducted due to the lack of disseminated flight test results. By inspecting for regimes well outside Saab 2000's operational Mach number and lift coefficient envelope, deviations in the total drag were quantified and qualitatively reviewed for relevant conclusions. At relatively low free stream Mach numbers and lift coefficients approximately 1.5 times higher than maximum operational values, and for Mach numbers in excess of the vehicle's M_{mo} boundary, errors of between +2 to +5% resulted.

The presented investigation is just one salient example of prediction accuracy - combined with the more rigorous investigation⁽¹²⁾ indications show very good agreement

against published results with typical errors frequently falling within a bandwidth of $\pm 5\%$ for weight, aerodynamics and performance. Additionally, the QCARD package was also utilised for two Saab Aircraft AB conceptual design studies and these exercises verified the accuracy of field-enroute performance and OTPA trajectory-profile generation algorithms previously discussed.

Aircraft Optimisation

The General Approach

Since it has been shown that computational effort has been minimised without undue loss of detail and precision in the result, it is suggested that an approach which rids the designer of expending energy in formulating baselines or an initial balanced aircraft design would be prudent. By reducing almost all configuration related analysis to a baseline fuselage exterior and interior layout or "quasi-initial baseline" formulation, this leaves the technical judgement process to consider what arbitrary array of independent variables are to be varied and by what arbitrary interval quantities. Rather than improving on a known baseline candidate, the identification of a region of feasibility enables the designer to choose through intuition what configuration would suitably fulfil the specifications, or conversely, permit transparency by giving the opportunity of assessing the benefits which arise when initial specifications are relaxed. The interdependencies between free variables with regard to overall design sensitivity can become somewhat easier to interpret if the dependent variable is expressed as a tangible quantity, for example as operational performance, design weights, cost, profit, etc. instead of traditional intermediary mainstays like drag, lift coefficient or aspect ratio.

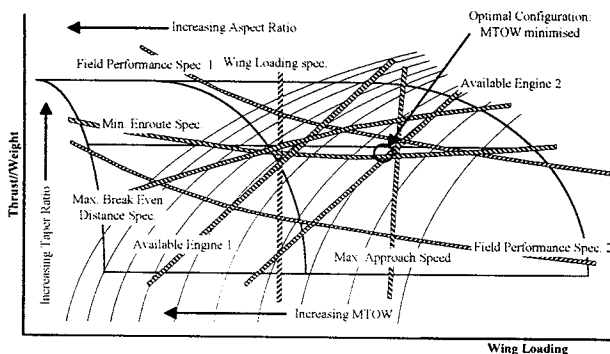


FIGURE 6 - Example of typical arbitrary free variable sensitivity study and subsequent identification of optimal configuration.

Conceptual Aircraft Design Problem

Growing public apprehension has created a preference for turbofan aircraft to assume the traditional regional role supported by turboprops. The market also has increasing interest in small regional jets not only to enlarge the catchment area in the hub and spoke system but more

importantly to create possibilities of entering a new direct services market or avoiding congested hubs thereby filling new niche markets of mid-length and long thin routes abandoned by major airlines. The pundits had forecast a radical shift away from turboprops for the 50 seater category and current indications show this to be accurate; as spectacularly exemplified by the successes of Canadair Regional Jet CRJ100 and Embraer RJ145.

In view of these events, the focus is now concentrated on the 30-35 passenger category with the introduction of Dornier Do328-300 and Embraer RJ135 vehicles. Unlike their 50 passenger turbofan counterparts these aeroplanes are not truly optimised vehicles but are reconfigured versions with great emphasis placed on economic considerations of commonality. The most unfortunate consequence of this situation is that the contemporary 30-35 passenger turbofan has become quite limited in terms of operational flexibility and large penalties with regards to the field-enroute performance and design weight trade off have been incurred. The goal of this project is to create a regional commuter aeroplane capable of demonstrating greater operational flexibility whilst still retaining the family concept philosophy as well as possessing a competitive operating costs edge.

After studying the current market the following specifications were formulated:

1. 30-35 seats at 32-31 inch seat pitch;
2. Engines to be new generation Williams FJ44-XX preliminary design fan with projected maximum sea level static thrust of 2850 lb.f. (12.68 kN);
3. JAR/FAR takeoff balanced field length of no greater than 5000 ft (1524 m) at ISA, sea level;
4. No climb restrictions on maximum takeoff gross weight for conditions up to and including ISA+30°C and 5000 ft airport elevations;
5. The penalty in off-loaded weight from MTOW to be significantly lower than competition when clearing FL 160 during OEI enroute climbs at ISA+20°C conditions (driftdown proficiency);
6. Minimum range of about 500 nm with full payload and an emphasis placed on maximising multi-hop capability for typical sector mission segments;
7. Comparable block times for typical sector missions with operating costs equal to or better than direct competitors;
8. Flexibility for both standard and extended-range versions; and
9. A derivative of the 19 PAX PD340-2 tri-jet turbofan vehicle⁽¹³⁾ with an emphasis placed on maximising commonality.

Initial Design and Sensitivity Analysis

The basic shape of the aircraft was already set because a specification to adhere to a family concept was proposed. The initial trade study involved inspection of different stretched fuselage layouts until both cargo and seating could be maximised with respect to general performance

criteria and powerplant used.

An example of the final trade study for PD340-3X STD is given in Figure 7. In this particular instance, since the powerplant was already selected, Maximum TakeOff Gross Weight (MTOGW) was traded against reference wing area with off-loaded fuel (maximum available fuel less some arbitrary fixed amount) as the additional primary sensitivity parameter. The reference wing area trade interval was not large due to a stipulation given by the specifications of utilising already existing structure: the PD340-2 wing imposed limitations on maximum span increase through introduction of a minimum permissible taper ratio threshold of $\lambda \geq 0.27$ set by the author. Even though guidelines for cost and profit optimisation were available, initial observations showed that fixed sector mission performance parameters like block time and block fuel did not alter by any great measure due to this small reference wing area interval thus not affording much scope for assessment of operational flexibility versus DOC and ROI. It was therefore postulated that cost would in this instance show an adequate measure of potential for profitability and was then in turn considered to be a direct function of airframe weight - this assumption having the additional benefit of minimising the effort expended for final selection. The selection process for optimum MTOW and corresponding wing reference area necessitated a trade off between increases in range and OEI climb performance against minimising of balanced field length (BFL) together with the landing reference speed (v_{ref}) or indirectly the required landing distance. Attention should be paid to the constraints shown in Figure 7. They represent maximum

maximum attainable stage length (MT-MS) assuming minimum time flight techniques with various passenger mission requirements and JAR OPS-1 reserves, and finally, off loaded weight penalties from MTOGW associated with lines indicating clearance of FL 160 assuming ISA+20°C conditions and one engine inoperative (OEI). The v_{ref} speed constraint lines were derived by assuming that each respective candidate completes a stage length of 200 nm from MTOGW at brake release and finishes with a conservative landing gross weight based on fuel burned via minimum fuel techniques - in accordance with the multi-hop specification. The optimum reference wing area was chosen to be 31.77 m² (342 sq. ft) which corresponds to a predicted MTOW of 12950 kg (28550 lb) defined by the criterion that 1369 kg (3018 lb) of fuel is off-loaded from its respective maximum available fuel load of 2912 kg (6420 lb).

Design Description

As discussed, the already existing PD340-2 wing planform was utilised and subsequent optimisation involved span increases with some modifications to wing tip geometry. Span is increased from the current 15.24 m (50 ft) to 17.88 m (58 ft 8 in.) with PD340-2's basic wing planform intact. The span increase gives a 9% wing area expansion (and 8% greater maximum available fuel capacity) with associated increases in aspect ratio from 8 to 10 and flap as well as aileron span. A moderate sweepback combined with a relatively thick supercritical wing section profile enables cruise Mach numbers in the region of 0.70-0.75 while projected certification altitude remains at 35000 ft. The wing planform geometry has been enhanced through the introduction of raked wing tips which is envisaged to decrease induced drag at low speeds with the added advantage of reducing wetted area to a smaller extent. The PD340-2's high lift system of double slotted Douglas type flaps have been retained and are expected to deliver slightly higher ΔC_L when deployed for PD340-3X due to improved aerodynamic efficiency.

The fuselage cross section has not been altered from the basic PD340-2 which was incidentally based on dimensions used for the Saab 2000 and Saab 340 vehicles. The structure itself has been stretched from original 16.70 m (54 ft 9 in.) used for the 19 PAX to 19.20 m (63 ft) for the 31-34 PAX variant. There is space for 31 passengers at a comfortable 32 inch seat pitch, or alternately, 34 passengers can be seated at a 31 inch pitch. Due to the larger capacity of this vehicle, additional space has been incorporated to the PD340-2's cargo hold resulting in an increase from 6.4 m³ (25 cu. ft) to 8.3 m³ (295 cu. ft).

The nacelles have also been modified since the fan is slightly larger and airflow requirements are higher. Projected increases in fan diameter with the Williams preliminary design FJ44-XX compared to PD340-2's already existing FJ44-2 installation are approximately 0.76 m (3 in.). This fortuitously requires no lengthening of the landing gear legs but the gear must accommodate

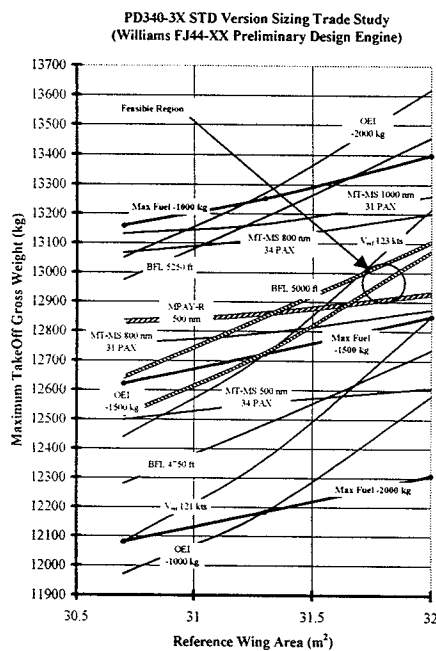


FIGURE 7 - Trade study and final configuration selection for PD340-3X STD tri-jet regional transport.

payload range (MPAY-R) assuming maximum SAR flight techniques and JAR OPS-1 reserves, lines of constant

increases in constituent weight due to overall increases in gross weight.

The increase in empennage moment arm is produced by a fuselage stretch, and calculations have shown that no changes to the PD340-2's existing empennage are necessary to cope with both the larger wing and higher thrust ratings of PD340-3X.

Predicted Performance and Design Review

Figure 8 gives a three-view representation while Table 1 summarises the predicted PD340-3X STD and PD340-3X ER weight, geometry and performance characteristics. It should be noted that the PD340-3X STD powerplant thrust has been derated to 2600 lb.f maximum static rating

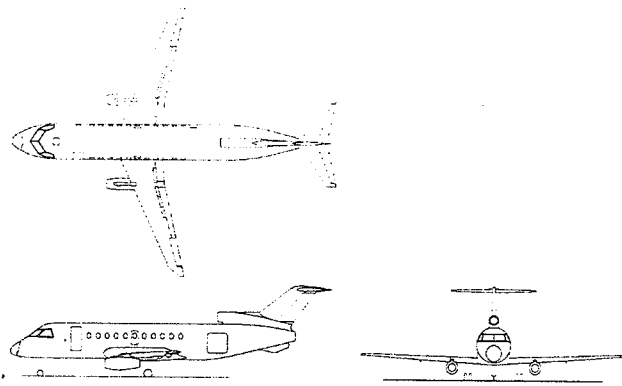


FIGURE 8 - PD340-3X 31-34 PAX regional tri-jet general arrangement.

whereas the PD340-3X ER utilises the maximum flat rating of 2850 lb.f at ISA, s.l., available from Williams' FJ44-XX preliminary design engine.

	PD340-3X STD		PD340-3X ER	
Weights				
Maximum Takeoff Weight	12950 kg	28550 lb	13750 kg	30313 lb
Maximum Landing Weight	12436 kg	27416 lb	13224 kg	29154 lb
Maximum Structural Payload	3720 kg	8201 lb	3720 kg	8201 lb
Geometry				
Wing Span	17.88 m	58 ft 8 in.	17.88 m	58 ft 8 in.
Reference Wing Aspect Ratio	10.0		10.0	
Reference Wing Area	31.77 m ²	342 sq. ft	31.77 m ²	342 sq. ft
Wing Quarter Chord Sweep	21°		21°	
Wing Aerofoil Section	root	16%	MS(1)-0313 (mod)	
	tip	12%	supercritical	
Fuselage Length	19.20 m	63 ft	19.20 m	63 ft
Fuselage Maximum Diameter	2.31 m	91 in.	2.31 m	91 in.
Performance (ISA)				
JAR/FAR 25				
Balance Field Length, s.l.	1507 m	4944 ft	1586 m	5203 ft
AEO Service Ceiling	FL 350		FL 350	
OEI Ceiling	FL 173		FL 191	
Typical Max. Cruise Speed	M0.72		M0.72	
JAR/FAR 25 Landing Distance				
without OEI braking	1480 m	4856 ft	1528 m	5013 ft
with OEI braking	1294 m	4245 ft	1341 m	4350 ft

TABLE 1 - Data for PD340-3X STD and PD340-3X ER.

Figure 9 shows the predicted payload-range for both standard and extended range versions of the aircraft. The chart curves are given for maximum SAR and maximum

block speed flight techniques since this representation not only gives the maximum range capability but also an indication of the maximum fixed sector distance performance afforded by the vehicle for given mission payload and assuming minimum time flight techniques. Comparison for typical sector missions of 34 PAX and stage length of 500 nm with JAR OPS-1 reserves policy and minimum time flight techniques in ISA still air show that PD340-3X is approximately 4 minutes slower than the Embraer RJ135 where the total block time for both aircraft is around 1 1/2 hours. This performance is complemented by a significant reduction in block fuel - an estimated saving of around 30% can be achieved with PD340-3X over its competitor. The TOGW required for completing this mission results in PD340-3X being approximately 4100 kg (9000 lb) lighter over RJ135 which exemplifies the projected lower airport charges through a MTOW review, and, the BFL comparison using these mission gross

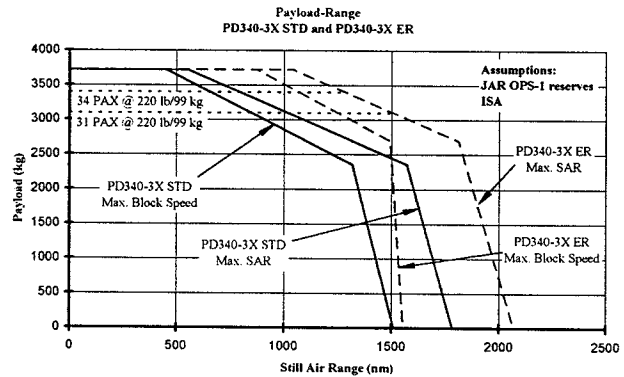


FIGURE 9 - Payload-range envelope for PD340-3X STD and PD340-3X ER 31-34 PAX regional turboprop transport.

weights are also in favour of PD340-3X with field lengths of 1291 m (4236 ft) at s.l., ISA for standard and extended range versions assuming an initial takeoff flap setting of 20°. This is approximately 6% shorter than RJ135 employing a 22° takeoff flap setting at similar ambient conditions. Direct comparison to Do328-300 could not be conducted owing to the lack of reliable detailed data, however, early indications show that this vehicle is slower in terms of block speed than both PD340-3X and RJ135 for fixed stage lengths but is superior in terms of field length performance. No climb limitations on MTOGW are imposed (assuming no field length limited unbalanced performance exists) for conditions up to ISA+35°C and ISA+29°C and 5000 ft airport pressure elevation for PD340-3X STD and PD340-3X ER vehicles respectively. This makes for competitive performance even if the Do328-300 is characterised by exceptional field climb performance. The RJ135 is climb limited for conditions above ISA+25°C and 2500 ft airport pressure altitude. Combined with a target acquisition cost of USD 7-8 million, this design is seen to be an attractive as well as competitive alternative to the contemporary 30-35 PAX turboprop vehicles in the market.

Conclusions

It has been demonstrated that conceptual design of modern transport subsonic aircraft need not be relegated for the sake of a reduction in complexity to the realm of first order closed expressions or coarser numerical integration procedures which are prone to large errors and poor objective function sensitivity against a generalised set of design parameters. By combining many of the discrete operations usually performed for a conventional design process with the single solution philosophy, designers can utilise both the intuitive and non-hierarchical approach to create a powerful method that dispenses with the need for MVO techniques. By adopting an attitude more attune to actual operational considerations, the methodology presented through transcendental functions has surpassed the closed form expression in complexity somewhat. Notwithstanding, the spreadsheet based software QCARD or Quick Conceptual Aircraft Research and Development which embodies this theory has demonstrated an appreciable reduction in programming complexity usually required for MVO whilst affording the designer complete control at all steps of the process and confronting them with issues of realistic operational concern. To demonstrate the accuracy of the method seven known aircraft designs ranging in size from 19 to 100 passengers were input and subsequently validated its predictive powers. A 31-34 PAX turbofan regional transport was designed and optimised in order to demonstrate the speed and comprehensiveness of the method and resulted in a vehicle which can be regarded as a competitive proposal against its contemporaries.

References

- ¹Abbott, I.H., Von Doenhoff, A.E., "Theory of Wing Sections", Dover Publications Inc., 1949.
- ²Boppe, C.W., "CFD Drag Predictions for Aerodynamic Design", AGARD Report AR-256, 1989.
- ³Canadair Regional Jet Performance Data, Model CL-601R, MAA-601R107F, Issue F, Bombardier, February 1993.
- ⁴Eckert, E.R.G., "Engineering Relations for Friction and Heat Transfer to Surfaces in High Velocity Flow", Journal of the Aeronautical Sciences, Vol. 22, 1955, pp. 585-587.
- ⁵Embraer RJ135 Technical Description, TD-135/000, November 1997.
- ⁶EMB145 Technical Description, TD-145/009, January 1997.
- ⁷Erzberger, H., Lee H., "Characteristics of Constrained Optimum Trajectories with Specified Range", NASA Technical Memorandum 78519, Ames Research Center.
- ⁸Fokker 70 Performance Information Rolls-Royce Tay Mk620 (metric units), MM100/AA/F70/P.I.R.-M/issue 2, Fokker Aircraft B.V., May 1993.
- ⁹Fokker 100 Performance Information Rolls-Royce Tay Mk650 (imperial units), MDAA/F100/RP-110 Issue 1, Fokker Aircraft B.V., January 1990.
- ¹⁰Gogate, S.D., Pant, R.K., Arora, P., "Incorporation of

Some Cost and Economic Parameters in the Conceptual Design Optimisation of an Air-Taxi Aircraft", AIAA-94-4301-CP, pp. 443-453.

¹¹Isikveren, A.T., "A Method to Identify Optimal Flight Techniques of Transport Aircraft", Report 98-7, Royal Institute of Technology, Department of Aeronautics, Sweden, September 1998.

¹²Isikveren, A.T., "Suggested Procedures in Conceptually Predicting Structural Weight and Low-Speed/Enroute Aerodynamics and Performance Attributes of Transport Aircraft", Report 98-6, Royal Institute of Technology, Department of Aeronautics, Sweden, September 1998.

¹³Isikveren, A.T., "The PD340-2 19 Passenger Turbofan Regional Transport-Feasibility Study", Report 98-5, Royal Institute of Technology, Department of Aeronautics, Sweden, September 1998.

¹⁴Linnell, R., "Weight Estimation Methods", FKHV-1-RL790724:01, Saab AB, July 1979.

¹⁵McCormick, B.W., "Aerodynamics, Aeronautics, and Flight Mechanics", John Wiley and Sons, 1979.

¹⁶Miller, L.E., "Optimal Cruise Performance", Engineering Notes, Journal of Aircraft, Vol. 30, No. 3, May-June 1993, pp. 403-405.

¹⁷Obert, E., "Some Aspects of Aircraft Design and Aircraft Operation", Lecture Series, Sweden, 1996.

¹⁸Raymer, D.P., "Aircraft Design: A Conceptual Approach", American Institute of Aeronautics and Astronautics, 1989.

¹⁹Saab 2000/AE2100A Performance Engineers' Handbook Metric Version, Revision B, 73ADS0394, Saab Aircraft AB, October, 1996.

²⁰Scott, P.W., Nguyen D., "The Initial Weight Estimate", SAWE Paper No. 2327, Index Category No. 11, MDC 96K0030.

²¹Simos D., Jenkinson L.R., "The Determination of Optimum Flight Profiles for Short-Haul Routes", Journal of Aircraft, Vol. 22, No. 8, August 1985, pp. 669-674.

²²Torenbeek, E., "Optimum Cruise Performance of Subsonic Transport Aircraft", Report LR-787, Delft University of Technology, Faculty of Aerospace Engineering, The Netherlands, March 1995.

²³Torenbeek, E., "Optimum Wing Area, Aspect Ratio and Cruise Altitude for Long Range Transport Aircraft", Report LR-775, Delft University of Technology, Faculty of Aerospace Engineering, The Netherlands, October 1994.

²⁴Torenbeek, E., "Synthesis of Subsonic Airplane Design", Delft University Press, The Netherlands, 1982.

²⁵Young, A.D., "The Aerodynamic Characteristics of Flaps", Aeronautical Research Council Reports and Memoranda, Ministry of Supply, United Kingdom, 1953.